NOTES AND CORRESPONDENCE

Improvements of an Ice-Phase Microphysics Parameterization for Use in Numerical Simulations of Tropical Convection

STEVEN K. KRUEGER, QIANG FU, AND K. N. LIOU

Department of Meteorology, University of Utah, Salt Lake City, Utah

HUNG-NENG S. CHIN

Lawrence Livermore National Laboratory, Livermore, California

8 November 1993 and 12 May 1994

ABSTRACT

It is important to properly simulate the extent and ice water content of tropical anvil clouds in numerical models that explicitly include cloud formation because of the significant effects that these clouds have on the radiation budget. For this reason, a commonly used bulk ice-phase microphysics parameterization was modified to more realistically simulate some of the microphysical processes that occur in tropical anvil clouds. Cloud ice growth by the Bergeron process and the associated formation of snow were revised. The characteristics of graupel were also modified in accord with a previous study. Numerical simulations of a tropical squall line demonstrate that the amount of cloud ice and the extent of anvil clouds are increased to more realistic values by the first two changes.

1. Introduction

Satellite imagery shows that large portions of the Tropics are covered by extensive cirrus anvil clouds (Liou 1986) associated with mesoscale convective systems. Recent GCM simulations show that tropical anvil clouds strongly influence both convection and the large-scale circulation of the atmosphere through their effects on the radiation budget and through the thermodynamical consequences of phase changes within clouds (Randall et al. 1989). The importance of tropical anvil clouds is also evident from the fact that the stratiform (anvil) rain accounts for 32%–49% of the total rain in the Tropics (Gamache and Houze 1983).

More realistic parameterizations of tropical anvil clouds are needed in GCMs (Randall et al. 1989). For studying cloud–radiation interactions and improving GCM cloud parameterizations, cumulus ensemble models (CEMs) are an important tool (Xu 1993). CEMs are cloud-resolving models used for relatively large-domain and long-time simulations. To study cloud–radiation interactions in tropical mesoscale convective systems with a CEM (or other numerical model that includes explicit cloud formation), the cloud properties that strongly affect the radiative fluxes, such as the extent and ice water content of anvil clouds, should be realistically simulated.

In cloud-resolving models used for simulating tropical convection, microphysical processes are most commonly parameterized following the bulk method with the hydrometeors categorized into five types: cloud droplets, raindrops, ice crystals, snow, and hail or graupel (McCumber et al. 1991). For several years, the bulk ice-phase microphysics code developed by Lord et al. (1984) and based on Lin et al. (1983) has been used in the 2D University of California, Los Angeles (UCLA)–University of Utah CEM (UU CEM) (Xu and Krueger 1991; Xu et al. 1992). Lord et al. generally followed Lin et al. except that they modified the density of graupel and the intercept parameter of rain to represent conditions in hurricanes better.

McCumber et al. (1991) compared simulations of tropical convection using the Lin et al., Lord et al., and Rutledge and Hobbs (1984) microphysical parameterization schemes. They compared some features of the simulated convection (the anvil portion of the surface rainfall and the intensity of the radar bright band) to observations. They found that for the three-ice-class schemes, the optimal mix of bulk ice hydrometeors is cloud ice–snow–graupel.

We have extended McCumber et al.'s study by examining the extent and ice water content of tropical anvil clouds simulated by the UU CEM using the Lord

Corresponding author address: Prof. Steven K. Krueger, Dept. of Meteorology, University of Utah, Salt Lake City, UT 84112.

et al. microphysics code. We find that the extent of the anvil clouds is underpredicted and that the cloud ice content is too low compared with observations (Houze and Betts 1981; Ackerman et al. 1988). Lord et al. noted that parameterization of nucleation and subsequent growth processes for cloud water and cloud ice is an extremely difficult task because these processes are highly dependent on temperature, local supersaturation, droplet size, and crystal habit. Consequently, it is currently impractical to predict the detailed evolution of the cloud water and cloud ice fields in cloud-resolving models. However, improvements can be made within the framework of Lord et al.'s microphysics parameterization to simulate a more realistic cloud ice distribution in tropical anvil clouds for radiative heating calculations.

In the next two sections, we describe our modifications to Lord et al.'s parameterizations of cloud ice growth by the Bergeron process and snow formation associated with the Bergeron process. In section 4 we document the changes we made to Lord et al.'s graupel parameters based on McCumber et al.'s results. In section 5 we compare the anvil extent, hydrometeor evolution, and hydrometeor profiles in two simulations of a tropical squall: one with Lord et al.'s original microphysics code, and one with our modified version. The results are summarized in section 6.

2. Growth of cloud ice by the Bergeron process

In Lord et al.'s parameterization, cloud ice increases due to nucleation and depositional growth and decreases due to sublimation, conversion to snow, and accretion by snow and graupel. The interactions among cloud water, cloud ice, and water vapor due to condensation/evaporation, deposition/sublimation, melting of cloud ice ($T \geq 0°C$), and homogeneous freezing of cloud water ($T \leq -40°C$) are represented by a "saturation adjustment" scheme and a simple model of the Bergeron process.

A saturation adjustment scheme is based on the assumption that all supersaturated vapor condenses or deposits. Lord et al. introduced a generalized saturation adjustment scheme for cloud water and cloud ice. In their scheme, the saturation mixing ratio is defined as the mass-weighted average of the respective saturation values over liquid water and ice when both cloud water and cloud ice are present. All supersaturated water vapor is partitioned between cloud water and cloud ice as a linear function of temperature between 0° and 40°C.

The Bergeron process represents the vapor depositional growth of cloud ice or snow at the expense of cloud water in supercooled clouds ($-40°C \leq T \leq 0°C$), which are saturated with respect to water and, therefore, supersaturated with respect to ice due to the difference in saturation vapor pressures of ice and water. This process cannot be accounted for by a saturation adjustment scheme. The Bergeron process for cloud ice in Lord et al. (I_{dw}) is based on the formulation by Lin et al. (P_{IDW}), which follows that of Hsie et al. (1980) (P_{CNWD}). We will use Lin et al.'s notation henceforth.

The growth rate of cloud ice due to nucleation and the Bergeron process (P_{IDW}) is based on the growth rate of ice crystals with the mass of a natural ice nucleus (1.05×10^{-15} g) and a number concentration equal to the number of natural ice nuclei. The growth rate of a single crystal, as parameterized by Koenig (1971), is

$$\frac{dm_i}{dt} = a_1 m_i^{a_2},$$

where m_i is the ice crystal mass, and a_1 and a_2 are positive temperature-dependent coefficients tabulated by Koenig, where a_2 ranges from about 0.4 to 0.6. The mass of a natural ice nucleus is much smaller than a typical ice crystal mass. In our modified formulation, instead of the ice nucleus mass, we use the average mass of an ice crystal, which is estimated to be

$$m_i = \frac{q_i \rho_a}{N_n},$$

where q_i is the mixing ratio of cloud ice, ρ_a is the density of air, and N_n is the number concentration of active natural ice nuclei (Fletcher 1962).

To verify that this modification better represents the Bergeron process, a rising-parcel model was used along with Lord et al.'s saturation adjustment and P_{IDW} in its original and modified forms. The results are compared to those produced by a more realistic approach that explicitly calculates the condensation and evaporation of cloud water, the initiation of cloud ice, and the depositional growth of cloud ice (Rutledge and Hobbs 1983). The parcel is assumed to rise without mixing with its environment. The initial pressure, temperature, and mixing ratio of water vapor are taken to be 559 mb, 270 K, and 2.1 g kg^{-1}, respectively. The parcel moves upward with a speed of 0.02 mb s^{-1} and at the same time the pressure in the parcel adjusts to the ambient pressure. A 25-s time step was used in model simulations.

Figure 1 shows the parcel model results for the mixing ratios of water vapor, cloud water, and cloud ice as a function of time using (a) the original Lord et al. formulation, (b) the modified formulation, and (c) the Rutledge and Hobbs formulation. The depositional growth of cloud ice at the expense of cloud water is insignificant when using the original Lord et al. formulation (Fig. 1a). Results computed using the modified ice crystal mass (Fig. 1b) show much better agreement with the results obtained using Rutledge and Hobbs' approach (Fig. 1c). After 350 time steps, the mixing ratio of cloud water becomes zero in Fig. 1b due to the Bergeron process. The slight differences between Figs. 1b and 1c are attributed to the different mechanisms of cloud ice initiation in the two schemes.

3. Snow formation associated with the Bergeron process

The parameterized Bergeron process just described also produces snow from cloud ice via the growth of

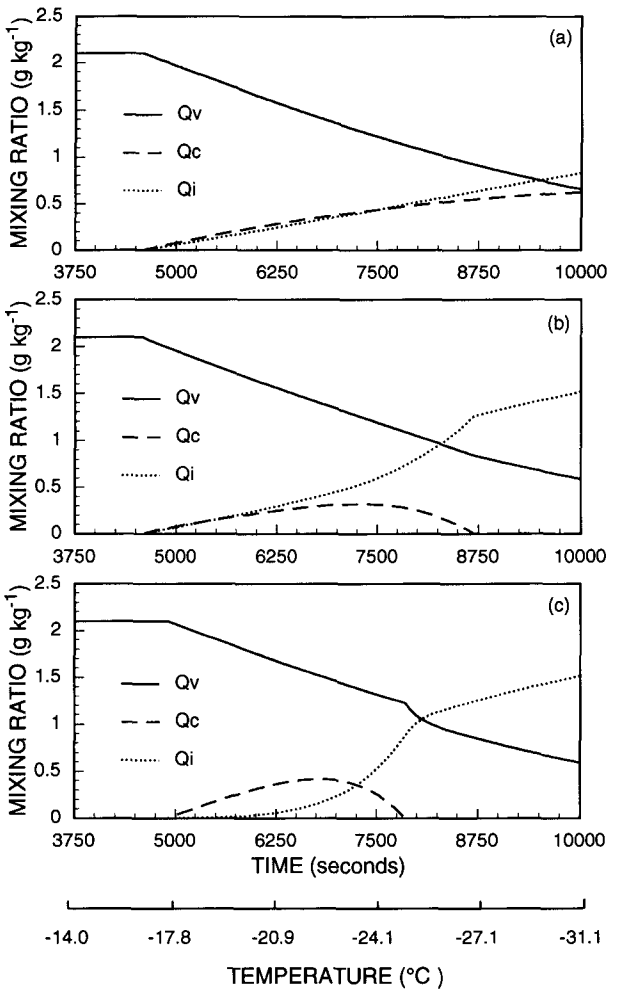

FIG. 1. Parcel model results for the mixing ratios of water vapor, cloud water, and cloud ice as a function of time using (a) the original Lord et al. (1984) formulation, (b) the modified formulation, and (c) the Rutledge and Hobbs (1983) formulation.

Bergeron-process embryos (P_{SFI}) and from cloud water via the Bergeron process and riming (P_{SFW}). Hsie et al. and Lin et al. expressed P_{SFI} and P_{SFW} as

$$P_{SFI} = \frac{q_i}{\Delta t_1}, \tag{1}$$

and

$$P_{SFW} = N_{ir}(a_1 m_{ir}^{a_2} + \pi \rho_a q_c r^2 U_{ir}),$$

where Δt_1 is the timescale needed for a crystal to grow from radius r_0 to radius r given by

$$\Delta t_1 = \frac{1}{a_1(1 - a_2)} [m_{ir}^{(1-a_2)} - m_{ir_0}^{(1-a_2)}],$$

where q_c is the mixing ratio of cloud water, and m_{ir} and U_{ir} are the mass and terminal velocity of an ice crystal with radius r. The number concentration of ice crystals with radius r is

$$N_{ir} = \frac{q_i \Delta t}{m_{ir} \Delta t_1},$$

where Δt is the time step in the numerical simulation.

Equation (1) indicates that the timescale Δt_1 determines the rate at which cloud ice is converted to snow. In their expressions for P_{SFI} and P_{SFW}, Lin et al. used a timescale for a crystal to grow from $r_0 = 40$ μm to $r = 50$ μm, which is somewhat artificially set (Hsie et al. 1980). Based on in situ aircraft observations, the mean effective sizes of ice crystal size distributions in ice clouds range from 24 to 124 μm (Fu and Liou 1993), which correspond to area-equivalent effective radii from 14 to 126 μm. Therefore, it is more realistic to define Δt_1 as the time needed for an ice crystal to grow from 40 to 100 μm and to determine P_{SFW} based on a 100-μm-radius ice crystal. Note that 40 μm is smaller than the median, and that 100 μm is smaller than the upper bound of the observed range of mean effective radii because very small ice crystals (<20 μm) cannot be observed by present optical probes. The maximum q_i obtained using the new timescale in the parcel model is about three times larger than obtained using the original timescale.

Cloud ice continues to be converted to snow by P_{SFI} in Lord et al.'s formulation even when there is no cloud water. Since Lord et al. assumed that cloud ice does not fall but snow does, P_{SFI} in this case acts like a crude fall-speed parameterization for cloud ice. To validate this approach, it should be compared to a detailed parameterization of ice crystal fall speeds.

4. Graupel characteristics

For tropical cumuli over the oceans, McCumber et al. concluded that it is better to choose the bulk ice hydrometeor mix to be cloud ice–snow–graupel rather than cloud ice–snow–hail. In their numerical simulations of tropical convection, graupel, with a small terminal velocity, produced more realistic dynamic, thermodynamic, and radar characteristics of anvil clouds than did fast-falling hail. In particular, McCumber et al. found that choosing graupel parameters rather than hail parameters for the graupel–hail class of precipitating ice produced more realistic radar bright bands in tropical squall-line simulations. Therefore, we now use the intercept parameter n_0 and density ρ for graupel given by Rutledge and Hobbs (1984): $n_{0G} = 4 \times 10^6$ m^{-4} and $\rho_G = 0.4 \times 10^3$ kg m^{-3}. Lord et al. used $n_{0G} = 4 \times 10^4$ m^{-4} and $\rho_G = 0.3 \times 10^3$ kg m^{-3}. The most significant difference is in the intercept parameter. Rutledge and Hobbs' graupel parameters result in lower mass-weighted fall speeds. Lord et al.'s n_{0G} value is actually more representative of hail. This is evident in McCumber et al.'s reported average terminal velocities for graupel/hail for the three schemes: Lin et al. (hail), 10.2 m s^{-1}; Lord et al., 7.0 m s^{-1}; and Rutledge and Hobbs (graupel), 2.5 m s^{-1}.

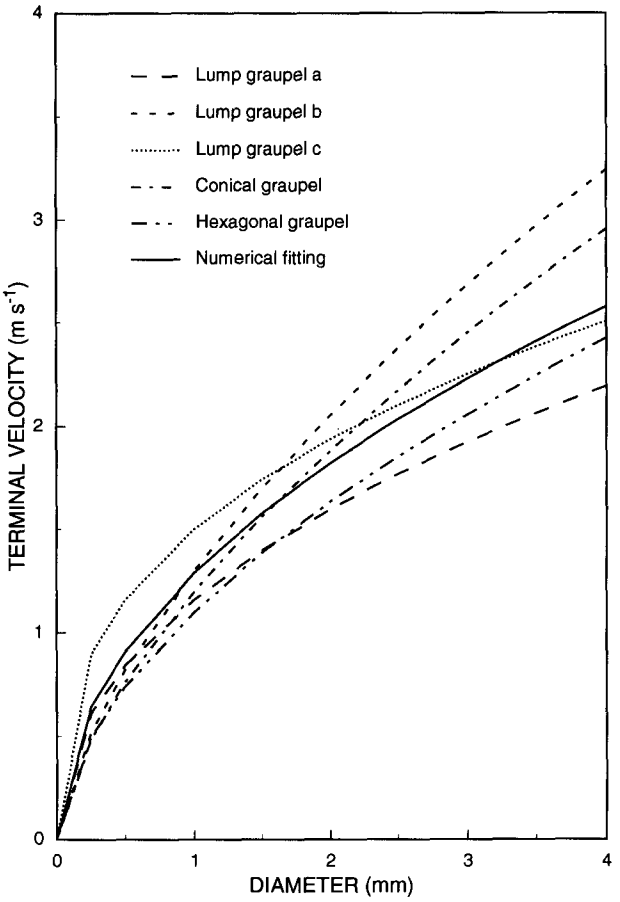

FIG. 2. Fall speed versus diameter for five different graupel types based on the velocity–size relationships given by Locatelli and Hobbs (1974). Using numerical fitting, we obtained an average relationship: $V_G = 1.288D^{0.5}$, where the units for V_G and D are meters per second and millimeters, respectively. The fall speed versus diameter curve based on the fitting is also shown.

We use the intercept parameter for rain given by Lin et al., $n_{0R} = 8 \times 10^6$ m^{-4}, in place of that used by Lord et al. (which is more appropriate for tropical cyclones), $n_{0R} = 22 \times 10^6$ m^{-4}. The snow parameters are unchanged from Lord et al.'s: $n_{0S} = 3 \times 10^6$ m^{-4} and $\rho_S = 0.1 \times 10^3$ kg m^{-3}.

The terminal velocity that we use for graupel was determined from measurements reported by Locatelli and Hobbs (1974). Figure 2 shows fall speed versus diameter curves for five different graupel types based on the velocity–size relationships given by Locatelli and Hobbs. The fall speed–diameter relation used by Rutledge and Hobbs (1984) is for "lump graupel c." We expect that the average relationship is more suitable for a microphysics parameterization. Using numerical fitting, we obtained an average relationship as follows: $V_G = 1.288D^{0.5}$, where the units for V_G and D are meters per second and millimeters, respectively. The fall speed versus diameter curve determined from the above equation is also shown in Fig. 2.

Following Rutledge and Hobbs (1984), the collection efficiencies of snow for cloud ice and of graupel for snow ($T < 0$°C) are both set to 0.1. These values are a better match to the measurements presented by Lin et al. (in their Fig. 4) than the collection efficiencies used by Lin et al. Also, the thresholds for cloud ice and snow aggregation we use are 0.6×10^{-3} and 1.0×10^{-3}, instead of 1.0×10^{-3} and 0.6×10^{-3} as reported by Lin et al. (1983). There is an error in the units of a_1 in Hsie et al. (1980). The units should be g$^{1-a_2}$ s^{-1} in order to agree with Koenig (1971). There are also errors in Eqs. (43) and (47) in Lin et al. (1983). The denominator $3C_D$ should be multiplied by ρ in each.

5. Numerical simulations and results

We used the UU CEM to perform two simulations of an idealized tropical squall line to assess the effects of our modifications to the microphysics parameterization. One simulation used Lord et al.'s original microphysics scheme while the other used the modified microphysics scheme described in the previous section. The UU CEM is described in Krueger (1988) and Xu and Krueger (1991). For the two tropical squall-line simulations, we used a large horizontal domain in order

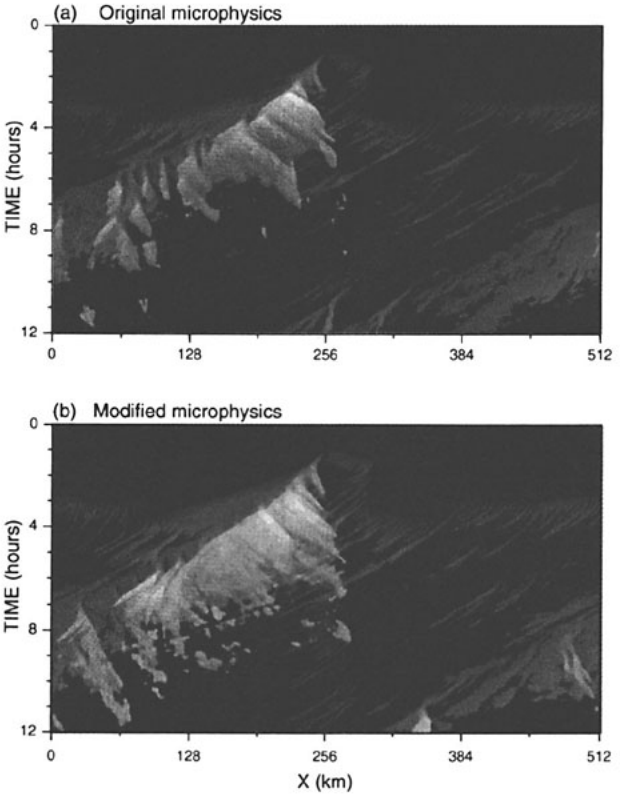

FIG. 3. Hovmöller (x–t) diagrams of cloud-top temperature from the simulations with (a) Lord et al.'s original microphysics scheme and (b) the modified scheme. The temperature is indicated by a linear gray scale from 300 K (black) to 200 K (white).

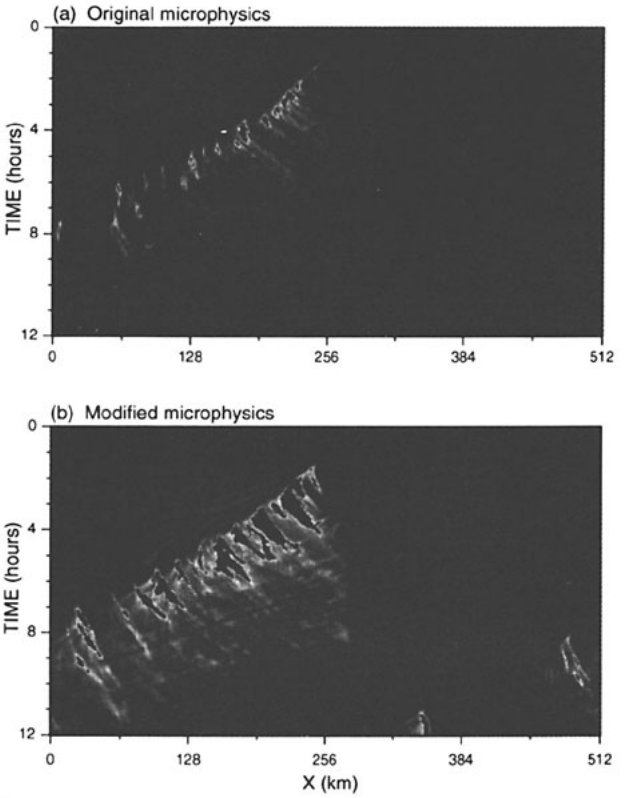

FIG. 4. Hovmöller (x–t) diagrams of the vertically integrated cloud ice content from the simulations with (a) Lord et al.'s original microphysics scheme and (b) the modified scheme. The ice content is indicated by a linear gray scale from zero (black) to 0.5 kg m^{-2} (white). In the black regions enclosed by white, the ice content exceeds 0.5 kg m^{-2}.

to include an extensive anvil. The domain is 512 km wide with a horizontal grid size of 1 km. The depth of the domain is about 19 km with a stretched coordinate consisting of 33 layers. Near the surface the vertical grid size is 100 m, while near the model top it is 1 km. The initial thermodynamic state is based on the GATE phase III mean sounding. The geostrophic (and initial) horizontal wind profile normal to the squall line is similar to the one used by Xu et al. (1992) in their simulation Q04 and resembles squall-line profiles observed during GATE phase III. We used the same large-scale advective cooling and moistening profiles as were used in simulation Q04. Each simulation was for 12 h. The squall line was initialized by a low-level cool pool (Tao et al. 1991) after 1 h. In each simulation, the large-scale forcing was constant for the first 4 h, decreased to zero during the next 4 h, and then remained zero for the last 4 h.

Figure 3 shows Hovmöller (x–t) diagrams of cloud top temperature from the simulations with (a) Lord et al.'s original microphysics scheme and (b) the modified scheme. The temperature is indicated by a linear gray scale: white represents 200 K, while black denotes 300 K. The cloud-top temperature is defined here as the temperature at the first level for which the mass of "suspended water" integrated downward from the model top exceeds 0.1 kg m^{-2}. Suspended water includes cloud water, cloud ice, and snow. Anvil clouds associated with the squall lines appear bright in Fig. 3. Because snow is included in suspended water, the differences between the two simulations are less dramatic than they would be if snow was not included. Despite this, the anvil cloud displayed in Fig. 3b (modified scheme) is still significantly more extensive than the one in Fig. 3a (original scheme). The maximum size of the anvil increased from less than 100 km (Fig. 3a) to about 180 km (Fig. 3b) due to the microphysics modifications. The typical anvil size observed during GATE was about 200 km (Houze and Betts 1981).

Hovmöller diagrams of the vertically integrated cloud ice content for the two simulations are shown in Fig. 4. In the black regions enclosed by white, amounts exceed 0.5 kg m^{-2}. Here the differences are dramatic: the modified scheme produces much more cloud ice than the original scheme. Amounts exceeding 0.5 kg m^{-2} are limited to the convective line with the

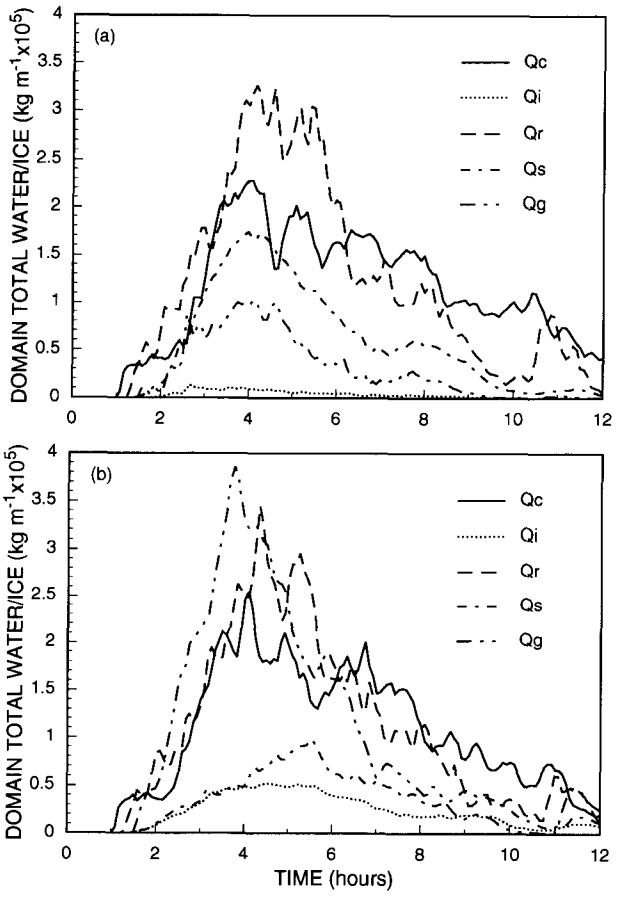

FIG. 5. Time series of domain total amounts of each hydrometeor species from the simulations with (a) Lord et al.'s original microphysics scheme and (b) the modified scheme.

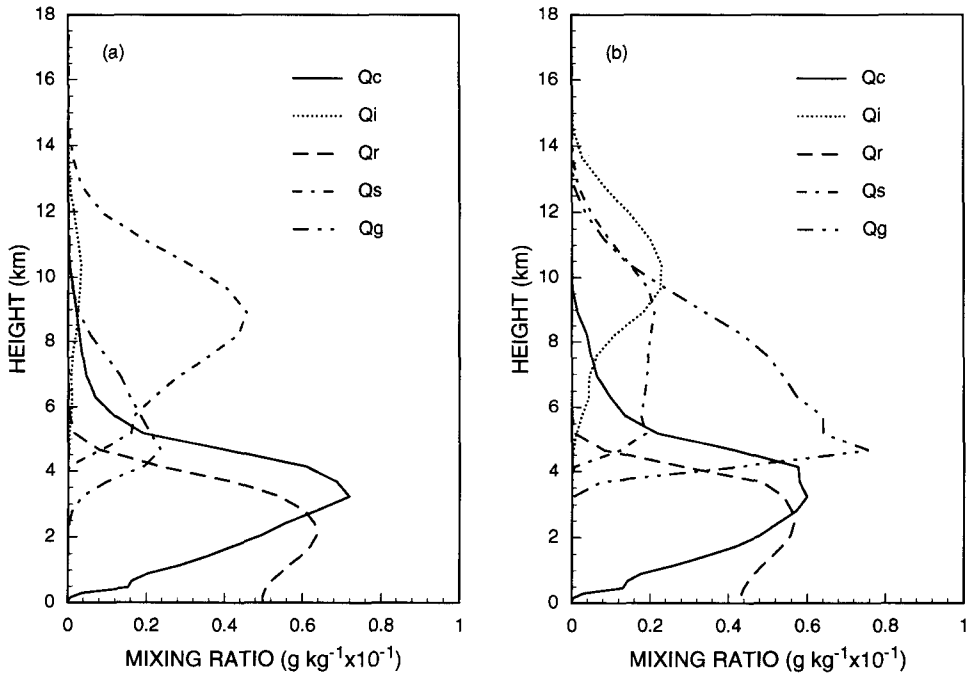

FIG. 6. Time and horizontally averaged mixing ratio profiles for each hydrometeor species from the simulations with (a) Lord et al.'s original microphysics scheme and (b) the modified scheme.

original scheme but extend about 50 km into the anvil with the modified scheme.

Fig. 5 shows time series of domain total amounts of each hydrometeor species for the two simulations. The cloud water and rainwater amounts do not differ significantly between the two. Cloud ice and graupel increase with the modified scheme, while snow decreases. In the original scheme, "cloud ice" represents small ice crystals, "snow" represents medium to large ice crystals plus aggregates, while "graupel" represents large, fast-falling ice particles. The result is small cloud ice amounts, large snow amounts, and small graupel amounts. In the modified scheme, "cloud ice" represents small to medium-sized ice crystals, "snow" represents large ice crystals, and "graupel" represents small, slow-falling ice particles (graupel and aggregates). The result is larger cloud ice amounts, lower snow amounts, and larger graupel amounts.

Figure 6 shows time and horizontally averaged mixing ratio profiles for each hydrometeor species for the two simulations. Lord et al.'s hydrometeor profiles in a mesoscale convective region of a tropical cyclone resemble ours using the original code (compare our Fig. 6a to their Fig. 6). The average cloud ice and graupel mixing ratios are larger with the modified scheme, and the average snow mixing ratios are less. Comparing our Fig. 6 to McCumber et al.'s Fig. 3 shows that changing the graupel parameters alone has a rather small effect on the average cloud ice mixing ratios compared to the modifications that we made to increase the anvil's extent and its cloud ice content.

The sum of the graupel and snow profiles in the upper troposphere in the modified case is similar to the snow profile in the original case. This suggests that the lower fall speed of the graupel in the modified scheme allows it to be carried to higher levels in the convective cores, from which it is expelled into the anvil cloud where it descends and grows by accreting snow. The graupel profile in the modified case has a sharp lower boundary where it melts. This produces a more realistic radar bright band than in the original case (McCumber et al. 1991).

The microphysical changes also affect the simulated squall-line dynamics. Analyzing these effects in detail is a worthy task for future research but is beyond the scope of this note. However, we did examine the gust front–relative horizontal velocity fields for both simulations averaged over the 2-h period from 6 to 8 h. We found that 1) the rear inflow jet is weaker but more extensive and deeper with the modified compared to the original microphysics, and that 2) the front-to-rear jet is also weaker with the modified compared to the original microphysics. The second result suggests that the more extensive anvil with the modified microphysics is not due to a stronger front-to-rear jet.

6. Summary

It is important to properly simulate the extent and ice water content of tropical anvil clouds in numerical models that explicitly include cloud formation because of the significant effects that these clouds have on the radiation budget. For this reason, the bulk ice-phase microphysics parameterization developed by Lord et al. (1984) and based on Lin et al. (1983) was modified to more realistically simulate some of the microphysical processes that occur in tropical anvil clouds. Cloud ice growth by the Bergeron process and the associated formation of snow were revised. The characteristics of graupel were also modified in accord with McCumber et al.'s (1991) conclusions. Numerical simulations of a tropical squall line demonstrate that the amount of cloud ice and the extent of anvil clouds are increased to more realistic values by the first two changes.

Acknowledgments. This research has been supported by AFOSR Grant 91-0039, NASA Grant NAG 5-1050, and the ARM program under the auspices of the DOE by the Lawrence Livermore National Laboratory under Contract W-7405-Eng-48. We thank Dr. N. Rao for assistance in preparing this manuscript and Dr. S. J. Lord for providing his microphysics code.

REFERENCES

Ackerman, T. P., K. N. Liou, F. P. J. Valero, and L. Pfister, 1988: Heating rates in tropical anvils. *J. Atmos. Sci.*, **45,** 1606–1623.

Fletcher, N. H., 1962: *The Physics of Rain Clouds.* Cambridge University Press. 390 pp.

Fu, Q., and K. N. Liou, 1993: Parameterization of the radiative properties of cirrus clouds. *J. Atmos. Sci.*, **50,** 2008–2025.

Gamache, J. F., and R. A. Houze, Jr., 1983: Water budget of a mesoscale convective system in the tropics. *J. Atmos. Sci.*, **40,** 1835–1850.

Hsie, E. Y., R. D. Farley, and H. D. Orville, 1980: Numerical simulation of ice phase convective cloud seeding. *J. Appl. Meteor.*, **19,** 950–977.

Houze, R. A., Jr., and A. K. Betts, 1981: Convection in GATE. *Rev. Geophys. Space Phys.*, **16,** 541–576.

Koenig, L. R., 1971: Numerical modeling of ice deposition. *J. Atmos. Sci.*, **28,** 226–237.

Krueger, S. K., 1988: Numerical simulation of tropical cumulus clouds and their interaction with the subcloud layer. *J. Atmos. Sci.*, **45,** 2221–2250.

Lin, Y. L., R. D. Farley, and H. D. Orville, 1983: Bulk parameterization of the snow field in a cloud model. *J. Climate Appl. Meteor.*, **22,** 1065–1092.

Liou, K. N., 1986: Influence of cirrus clouds on weather and climate processes: A global perspective. *Mon. Wea. Rev.*, **114,** 1167–1199.

Locatelli, J. D., and P. V. Hobbs, 1974: Fall speeds and masses of solid precipitation particles. *J. Geophys. Res.*, **79,** 2185–2197.

Lord, S. J., H. E. Willoughby, and J. M. Piotrowicz, 1984: Role of a parameterized ice-phase microphysics in an axisymmetric, nonhydrostatic tropical cyclone model. *J. Atmos. Sci.*, **41,** 2836–2848.

McCumber, M., W. K. Tao, J. Simpson, R. Penc, and S. T. Soong, 1991: Comparison of ice-phase microphysical parameterization schemes using numerical simulations of convection. *J. Appl. Meteor.*, **30,** 985–1004.

Randall, D. A., Harshvardhan, D. A. Dazlich, and T. G. Corsetti, 1989: Interactions among radiation, convection, and large-scale dynamics in a general circulation model. *J. Atmos. Sci.*, **46,** 1943–1970.

Rutledge, S. A., and P. V. Hobbs, 1983: The mesoscale and microscale structure and organization of clouds and precipitation in midlatitude cyclones. Part VIII: A model for 'seeder–feeder' process in warm-frontal rainbands. *J. Atmos. Sci.*, **40,** 1185–1206.

——, and ——, 1984: The mesoscale and microscale structure and organization of clouds and precipitation in midlatitude cyclones. Part XII: A diagnostic modeling study of precipitation development in narrow cold-frontal rainbands. *J. Atmos. Sci.*, **41,** 2949–2972.

Tao, W. K., J. Simpson, and S. T. Soong, 1991: Numerical simulation of a subtropical squall line over the Taiwan strait. *Mon. Wea. Rev.*, **119,** 2699–2723.

Xu, K.-M., 1993: Cumulus ensemble simulation. *The Representation of Cumulus Convection in Numerical Models, Meteor. Monogr.*, No. 46, K. A. Emanuel and D. J. Raymond, Eds., Amer. Meteor. Soc., 221–235.

——, and S. K. Krueger, 1991: Evaluation of cloudiness parameterizations using a cumulus ensemble model. *Mon. Wea. Rev.*, **119,** 342–367.

——, A. Arakawa, and S. K. Krueger, 1992: The macroscopic behavior of cumulus ensembles simulated by a cumulus ensemble model. *J. Atmos. Sci.*, **49,** 2402–2420.